Article

Cell Reports

Centriole Amplification in Zebrafish Affects Proliferation and Survival but Not Differentiation of Neural Progenitor Cells

Graphical Abstract

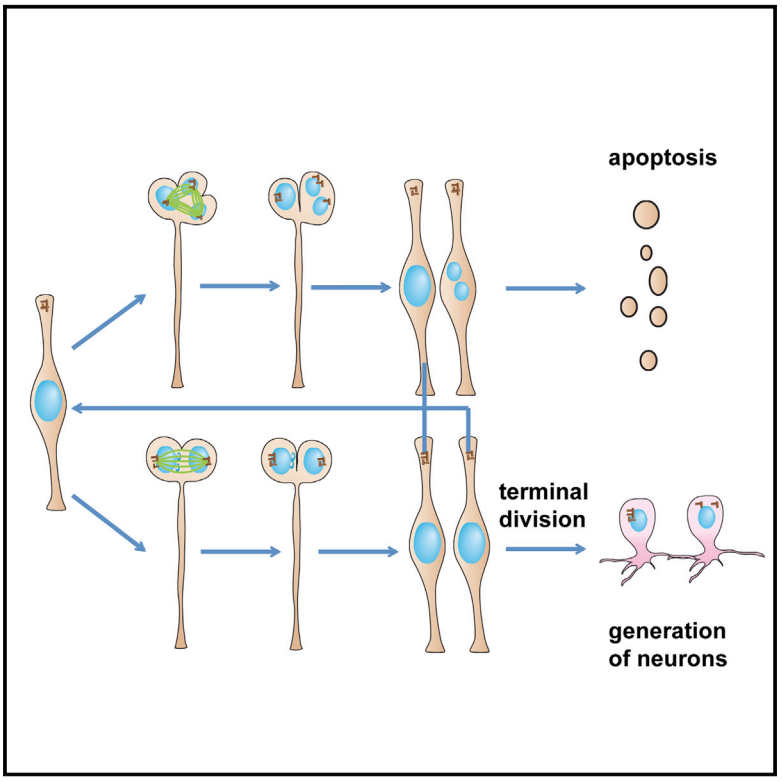

Authors

Edo Dzafic, Paulina J. Strzyz, Michaela Wilsch-Bräuninger, Caren Norden

Correspondence

paulina.strzyz@gmail.com (P.J.S.), norden@mpi-cbg.de (C.N.)

In Brief

Dzafic, Strzyz, et al. show that centriole amplification in neuroepithelia leads to apoptosis due to the generation of binucleated daughter cells upon multipolar divisions. If neurogenesis is reached before a cell enters apoptosis, cells can undergo timely differentiation into all retinal neurons. Interestingly, introduced control cells can compensate for apoptosis defects.

Highlights

- Centriole amplification causes significant apoptosis in zebrafish neuroepithelia
- Apoptosis is a specific consequence of the generation of binucleated cells
- Cells that did not die by apoptosis undergo timely differentiation into all retinal neurons
- Control cells can compensate for cell loss caused by centriole amplification

Dzafic et al., 2015, Cell Reports *13*, 168–182
October 6, 2015
http://dx.doi.org/10.1016/j.celrep.2015.08.062

OPEN ACCESS
CellPress

Cell Reports
Article

Centriole Amplification in Zebrafish Affects Proliferation and Survival but Not Differentiation of Neural Progenitor Cells

Edo Dzafic,[1,2] Paulina J. Strzyz,[1,2,*] Michaela Wilsch-Bräuninger,[1] and Caren Norden[1,*]
[1]Max Planck Institute of Molecular Cell Biology and Genetics, Pfotenhauerstraße 108, 01307 Dresden, Germany
[2]Co-first author
*Correspondence: paulina.strzyz@gmail.com (P.J.S.), norden@mpi-cbg.de (C.N.)
http://dx.doi.org/10.1016/j.celrep.2015.08.062

SUMMARY

In animal cells, supernumerary centrosomes, resulting from centriole amplification, cause mitotic aberrations and have been associated with diseases, including microcephaly and cancer. To evaluate how centriole amplification impacts organismal development at the cellular and tissue levels, we used the in vivo imaging potential of the zebrafish. We demonstrate that centriole amplification can induce multipolar anaphase, resulting in binucleated cells. Such binucleation causes substantial apoptosis in the neuroepithelium. Interestingly, not all epithelia are similarly sensitive to binucleation, as skin cells tolerate it without entering apoptosis. In the neuroepithelium, however, binucleation leads to tissue degeneration and subsequent organismal death. Notably, this tissue degeneration can be efficiently counterbalanced by compensatory proliferation of wild-type cells. Because the risk for generating a binucleated daughter recurs at every cell division, centriole amplification in the neuroepithelium is especially deleterious during progenitor proliferation. Once cells reach the differentiation phase, however, centriole amplification does not impair neuronal differentiation.

INTRODUCTION

Centrosomes are the major microtubule organizing centers in most animal cells. After cell division, cells contain one centrosome consisting of two centrioles, which are duplicated prior to mitosis, giving rise to two centrosomes (Meraldi and Nigg, 2002). Errors in the centriole duplication pathway, leading to the generation of more than two centrosomes consisting of more than four centrioles (centrosome/centriole amplification), can have severe consequences for cell division. It has been shown, both in vitro and in vivo, that supernumerary centrosomes can cause multipolar spindle formation. This, in turn, can result in the uneven distribution of genetic material and aneuploidy, leading to genetic instability and cancer propagation (Holland and Cleveland, 2012; Pihan et al., 2001). Moreover, human mutations in the centriole duplication pathway have been linked to microcephaly (Alderton et al., 2006; Nigg et al., 2014). Thus, gaining insight into how cells, tissues, and organisms respond to centriole and centrosome amplification has important implications for our understanding of a number of diseases.

Overexpression of the master regulator of the centriole duplication pathway, Polo-like kinase 4 (Habedanck et al., 2005), in both mouse (Plk4) and *Drosophila* (Sak) has been shown to lead to centrosome amplification. Interestingly, the effects of centrosome amplification can vary depending on the model organism studied and the tissue analyzed (Basto et al., 2008; Marthiens et al., 2013; Sabino et al., 2015). Fly neural precursors efficiently cluster supernumerary centrosomes. This results in bipolar spindle formation without major genetic distribution defects (Basto et al., 2008). No primary tumorigenesis is seen in the brain of these animals, and only if neural precursors are transplanted into adult hosts is tumor formation observed (Basto et al., 2008). In contrast, centrosome amplification in epithelial cells of the *Drosophila* larval wing disc induces multipolar spindles, and this is associated with apoptosis due to aneuploidy (Sabino et al., 2015). Mouse neural precursors behave similarly to *Drosophila* wing epithelial cells, as the induction of supernumerary centrosomes leads to abnormal distribution of genetic material. As in the fly wing, aneuploidy and cell death are common consequences of such aberrant divisions, in this case, leading to microcephaly. However, no tumor formation is observed in this tissue (Marthiens et al., 2013). Thus, the consequences of centrosome amplification appear to be highly context dependent.

To better understand the response of individual cells to centriole and centrosome amplification, it is important to analyze them in their normal in vivo context across a range of different tissues and organisms. Here, we exploit the in vivo imaging potential of the zebrafish to explore the consequences of centriole amplification. We find that centriole amplification in the zebrafish embryo leads to increased apoptosis in neuroepithelia. The primary cause of cell death is the formation of binucleated cells arising from multipolar segregation of genetic material in anaphase, followed by bipolar cytokinesis. In contrast, epidermal cells of the skin tolerate additional centrioles and binucleation without cell death. For the neuroepithelial cells, the risk of generating binucleated progeny recurs at mitosis of every

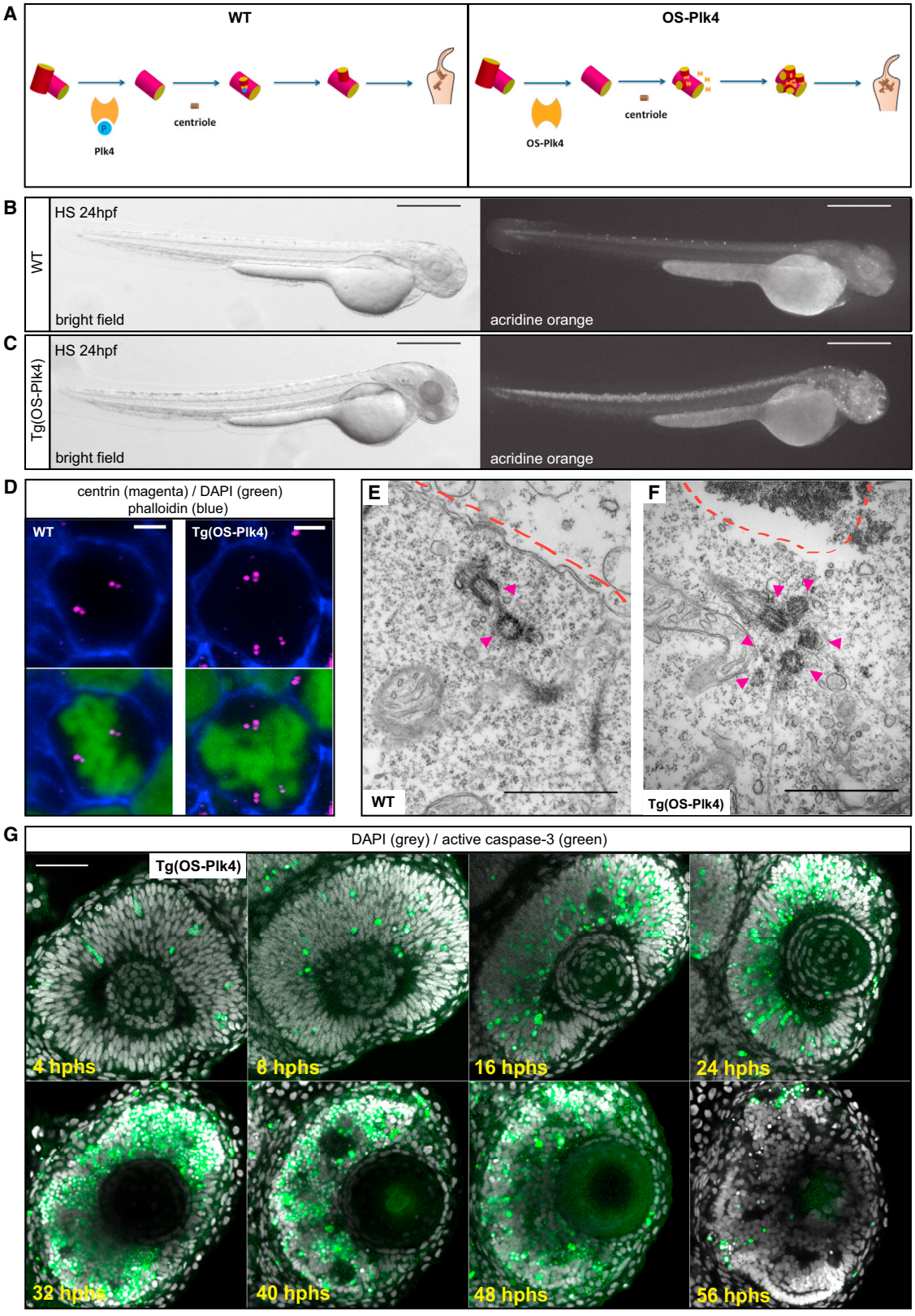

(legend on next page)

consecutive cell cycle. Accordingly, we find that proliferation, but not differentiation, is the bottleneck for successful tissue maturation upon centriole amplification. We further show that the presence of wild-type (WT) cells leads to significant compensation for apoptotic cell loss and thereby rescues some of the tissue abnormalities.

RESULTS

Expression of Overstabilized Plk4 Results in Centriole Amplification in the Developing Zebrafish

To achieve centriole amplification in the developing zebrafish, we expressed an overstabilized (OS) version of Plk4, the key regulator of the centriole duplication pathway, previously shown to induce supernumerary centrioles and centrosomes in cell culture (Holland et al., 2010) (Figure 1A). This construct was placed under a heat-shock (HS)-inducible promoter (Strzyz et al., 2015) to gain temporal expression control. A transgenic line was generated, in which, upon HS, all cells express OS-Plk4. Additionally, we introduced the HS-OS-Plk4-mKate2 construct via injection into one-cell-stage embryos to achieve mosaic OS-Plk4 expression.

To assess the global consequences of OS-Plk4 expression, we performed HS on transgenic embryos at 24 hr post-fertilization (hpf), when the overall body plan of the embryo is established and the development of major organs has been initiated (Kimmel et al., 1995). When embryos were inspected at 24 hr post-HS (hphs), dying tissue, especially in the eye and neural tube was detected, unlike in the controls. This cell death resulted in an overall reduction in eye and head size, and these organs were filled with darker tissue masses (Figures 1B, 1C, and S1A). Labeling with the apoptotic marker acridine orange revealed that OS-Plk4 expression led to a massive increase in apoptosis compared to the control (Figures 1B and 1C; N [number of embryos analyzed] = 20). The condition of transgenic embryos worsened until developmental day five when they stopped responding to external stimuli and eventually died (data not shown).

Next, we checked whether the phenotypes observed upon OS-Plk4 expression were, indeed, associated with centriole amplification. Antibody staining of mitotic retinal neuroepithelial cells revealed that more than two γ-tubulin/centrin-positive foci were frequently observed upon OS-Plk4 expression, while only two were seen in control cells (Figures 1D and S1B). This strongly suggested that OS-Plk4 expression induced the generation of supernumerary centrosomes. To confirm that these γ-tubulin and centrin-positive foci contain genuine centrioles, we performed electron microscopy (EM) on interphase neuroepithelial cells. We observed that the majority of control cells (N = 5, n [number of cells] = 31) featured two centrioles and never more than four (Figures 1E, S1C, and S2A). In contrast, 85% of OS-Plk4-expressing cells (N = 3, n = 20) exhibited four or more centrioles (Figures 1F, S1D, and S2A), and only 10% featured two centrioles. Taking into account that the process of centriole duplication continues until G2 (Fırat-Karalar and Stearns, 2014) and that, in the zebrafish neuroepithelium, G1 and S are the longest phases of the cell cycle (Leung et al., 2011), it is likely that, in many OS-Plk4 cases also, four centrioles already account for amplified centrioles. Together, this lets us argue that, upon OS-Plk4 expression, the majority of cells contained increased centriole numbers. To further validate this assumption, we performed en face imaging of the apical endfeet of mitotic neuroepithelial cells stained with anti-centrin2 antibody. In this case, in the WT scenario, the presence of two centrosomes, each consisting of two centrin-positive spots would be expected, as centrioles underwent a single round of duplication. This was, indeed, the case for the vast majority of control cells (Figure S2B; N = 5, n = 43). In the transgenic OS-Plk4 embryos, however, 90% of mitotic neuroepithelial cells (N = 9, n = 106) featured anomalies in centriole number and/or distribution and up to 10 centrin-positive foci per cell could be resolved (Figures S2B and S2C). Altogether, this shows that OS-Plk4 expression leads to the robust induction of centriole amplification in neuroepithelial cells. Additionally, we observed that expression of OS-Plk4 could induce a substantial variability of centriole numbers between cells, even within a single embryo (Figure S2D).

Having demonstrated that OS-Plk4 expression causes robust centriole amplification in neuroepithelial cells, we examined the resulting apoptotic phenotype in more detail. We performed anti-active-caspase-3 staining (Marthiens et al., 2013) and imaged embryos fixed every 8 hr from 4 hphs until 56 hphs. In the control, very few apoptotic cells were observed within this period (Figure S2F; N = 8). However, in OS-Plk4 transgenic embryos, a massive increase in apoptosis was observed between 8 and 16 hphs. The apoptotic outcome peaked between 24 and 32 hphs and was nearly completely resolved by

Figure 1. Expression of Overstabilized Plk4 in the Developing Zebrafish Induces Centriole Amplification and Subsequent Apoptosis

(A) Centriole duplication pathway in WT (left) and centriole amplification by expression of HS-inducible OS-Plk4 (right). The blue circle indicates a phosphate group. In the WT scenario, Plk4 is autophosphorylated and then degraded, leading to centriole duplication and four centrioles. OS-Plk4 lacks the phosphodegron domain; thus, it is not autophosphorylated and not degraded, leading to centriole amplification and multiple centrioles.

(B and C) A WT fish (B) and a transgenic (Tg)HS-OS-Plk4 fish (C). HS was applied at 24 hpf, and fish were imaged at 24 hphs/48 hpf and stained with acridine orange to label apoptotic cells. Left: bright field, right: acridine orange. Scale bars, 500 μm.

(D) Confocal scans, en face, of a mitotic WT neuroepithelial cell (left) with two poles, each containing two centrin spots (magenta) and a mitotic HS-OS-Plk4 neuroepithelial cell (right) with three poles: one featuring three centrin spots and two containing two centrin spots (magenta). Merged with cell outlines (phalloidin, blue) and chromatin (DAPI, green). Scale bars, 5 μm. HS was applied at 24 hpf, and cells were fixed at 16 hphs.

(E) EM image of a WT neuroepithelial cell showing two centrioles (magenta arrows). Dashed line marks the apical side. Scale bar, 1 μm. See Figure S1C for full series of sections. HS was applied at 24 hpf, and cells were fixed at 10 hphs.

(F) EM image of a Tg(HS-OS-Plk4) neuroepithelial cell showing six centrioles (magenta arrows). Dashed line marks the apical side. Scale bar, 1 μm. HS was applied at 24 hpf, and cells were fixed at 10 hphs.

(G) Time series of confocal scans of retinae of Tg(HS-OS-Plk4) fish. HS was applied at 24 hpf, and fish were stained for apoptotic marker active-caspase-3 (green) and DAPI (gray). Scale bar, 50 μm.

See also Figures S1B–S1D.

56 hphs (Figure 1G; N = 13–17). This apoptosis wave was less pronounced in injected embryos (Figure S2E; N = 5–8). Taken together, these results show that OS-Plk4 expression leads to increased apoptosis in neuroepithelia, resulting in tissue deterioration and, ultimately, organismal death. This is most likely due to the presence of supernumerary centrioles in OS-Plk4-expressing cells.

Centriole Amplification Leads to Bipolar and Multipolar Anaphases that Can Both Result in Aberrant Genetic Material Distribution

To investigate how OS-Plk4 expression and centriole amplification affect mitosis of neuroepithelial cells, we analyzed single-cell dynamics using mosaic expression of the chromatin marker H2B-RFP (red fluorescent protein) and the centrosome marker centrin-GFP (Strzyz et al., 2015). During interphase, all centrioles arranged into a single cluster localized to the apical surface and de-clustered only shortly before mitosis (Figures 2A and 2B; Movie S1). In some cases, multiple centrin-positive structures clustered into two poles, leading to bipolar separation of genetic material at anaphase (hereinafter referred to as bipolar anaphase) and the formation of two nuclei (Figures 2A and S4A; Movie S1). In other cases, the centrioles did not efficiently cluster and formed multiple (usually three) poles. This was followed by a multipolar separation of the genetic material at anaphase (multipolar anaphase) (Figure 2B; Movie S1). In both cases, "unbalanced" centrin signal was observed, with one pole appearing to have more centriolar material than the other (Figures 2B, S3A–S3D, and S4A–S4C; Movie S1).

Next, we quantified the number of bipolar and multipolar anaphases upon the injection of HS-OS-Plk4 and HS-H2B-RFP constructs. This analysis revealed that 65% of cells underwent a bipolar anaphase, and 35% underwent a multipolar anaphase (N = 20, n = 208). In the transgenic embryos, rates of multipolar anaphases reached 50% (N = 10, n = 150). Notably, no multipolar anaphases were observed in control cells (N = 13, n = 42).

Interestingly, OS-Plk4-expressing cells undergoing a multipolar anaphase completed cytokinesis with a single cytokinetic furrow, generating one daughter featuring two separate DNA masses (Figures 2C and 3G; Movie S2). We further showed by EM that each of the DNA masses featured a separate nuclear envelope (Figure 3A), meaning that multipolar anaphases lead to the generation of cells with two separate, non-diploid nuclei. Hereinafter, we will refer to these as binucleated cells.

To understand how cytokinesis occurs in these cells, we injected the actin marker HS-utrophin-GFP (Strzyz et al., 2015) and the chromatin marker HS-H2B-RFP, together with HS-OS-Plk4. Analysis of cytokinesis in these cells revealed that, despite the initiation of multiple cytokinetic furrows, cytokinesis was completed with a single furrow (Figure 2C; Movie S2).

To further investigate the dynamics of genetic material separation during multipolar and bipolar anaphases, we performed live imaging of cells injected with HS-OS-Plk4 at sub-minute resolution. In control cells, a clear metaphase plate was observed before the two nuclear masses were evenly distributed and moved toward opposite ends of the cell (Figure 3B; Movie S3). In contrast, OS-Plk4-expressing cells with a multipolar anaphase displayed abnormal chromosome dynamics, including bursts of chromatin out of the nuclear masses as well as lagging chromosomes (Figures 3C and 3E; Movie S3). This was followed by the formation of three chromatin masses, suggesting that cells undergoing multipolar anaphase encounter major problems with the distribution of genetic material. As it was previously proposed that cells undergoing a bipolar anaphase upon centriole amplification also show abnormalities in genetic material separation (Ganem et al., 2009), we wondered whether this was also the case in our system. Indeed, when cells exhibited bipolar anaphase, genetic material arrangements were similarly erratic, and no real metaphase plates were established (Figure 3D; Movie S3). Furthermore, lagging chromosomes could be detected (Figure 3F; Movie S3) and separated chromatin masses often appeared of unequal size (Figure 3D; Movie S3). Interestingly, despite these obvious problems in genetic material distribution, the length of mitosis in OS-Plk4-expressing cells was not particularly altered (Figure S4D).

Together, this shows that OS-Plk4 expression in neuroepithelial cells leads to defects in genetic material distribution. Upon a multipolar anaphase, the genetic material is distributed into three nuclear masses. Nevertheless, cytokinesis consistently leads to the formation of two cells, thus generating a binucleated daughter cell. Interestingly, unfaithful distribution of genetic material between two daughter cells can also be observed in cells exhibiting bipolar anaphases.

Cell Binucleation Leads to Apoptosis in the Neuroepithelium

To test whether apoptosis observed upon OS-Plk4 expression results from errors in genetic material separation, we followed single cells of HS-OS-Plk4-injected embryos. We quantified the apoptotic outcome of daughters generated after bipolar (N = 20, n = 134) and multipolar (N = 20, n = 74) anaphase by following cells for at least 3 hr after mitosis. To our surprise, we found that, despite the observed problems with chromatin distribution, very few daughter cells (4%) became apoptotic after bipolar anaphase (Figure S5A). Furthermore, only 16% of the mononucleated daughters arising from multipolar anaphases died. In contrast, 61% of binucleated daughters following multipolar anaphase died (Figure S5A; Movie S4) within 2 hr of mitosis completion (Figure 3I; Movie S4). We found similar trends in the transgenic line (N = 10, n = 94), in which 72% of binucleated cells underwent apoptosis, whereas cells that inherited one nucleus following multipolar anaphase, as well as daughters of bipolar anaphase, almost never entered the apoptotic program (Figure S5A). This result, together with our previous observation that mitoses upon OS-Plk4-induced centriole amplification feature defects in genetic material separation (Figures 3D and 3F; Movie S3), suggests that unfaithful distribution of genetic material does not automatically lead to cell death in the zebrafish neuroepithelium. Instead, apoptosis appears to be linked to the formation of binucleated cells.

Next, we checked whether apoptosis of cells was triggered by the p53 DNA damage response pathway, as shown upon centriole amplification in the mouse neocortex (Marthiens et al., 2013). We used previously established p53 morpholinos (Langheinrich et al., 2002) to deplete the protein. Interestingly,

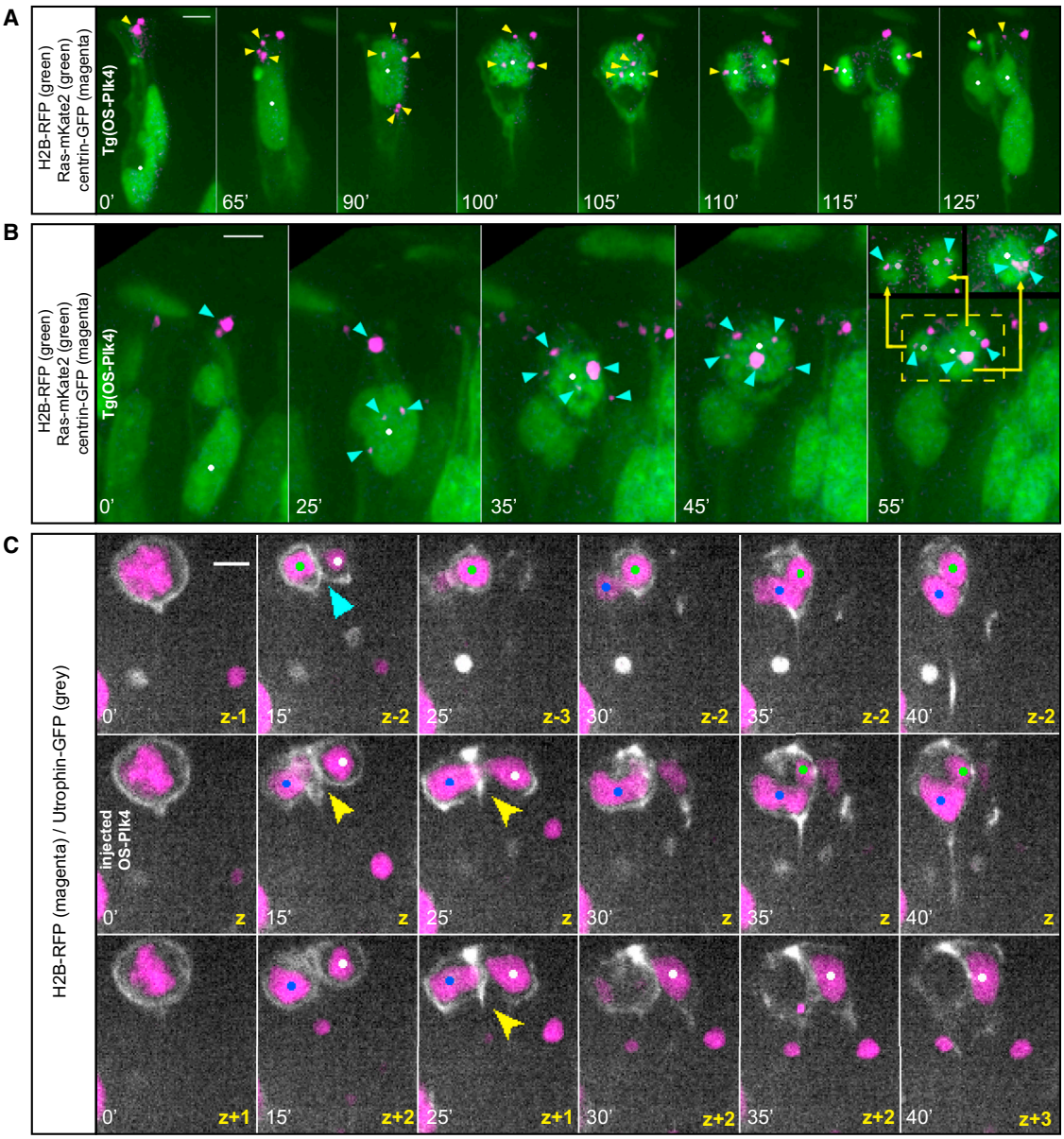

Figure 2. Centriole Amplification Induces Multipolar Anaphases but Bipolar Cytokinesis Generates Binucleated Progeny

(A) Time-lapse images of a neuroepithelial cell in a Tg(HS-OS-Plk4) embryo with a bipolar anaphase. H2B-RFP labels chromatin, Ras-mKate2 labels cell outline (both green), and centrin-GFP labels centrosomes (magenta). The yellow arrows mark the position of amplified centrioles (magenta). Nuclei are highlighted with dots. Frames are from Movie S1.

(B) Time-lapse images of a neuroepithelial cell in a Tg(HS-OS-Plk4) embryo with a multipolar anaphase. H2B-RFP labels chromatin, Ras-mKate2 labels cell outline (both green), and centrin-GFP labels centrosomes (magenta). The blue arrows mark the position of amplified centrioles (magenta). In the insets of the last frame. the daughter nuclei are shown in two different z planes to distinguish three separate nuclei. Nuclei are highlighted with dots. Frames are from Movie S1.

(C) Time-lapse images of a neuroepithelial cell during cytokinesis in three different z planes in an embryo injected with HS-OS-Plk4, HS-H2B-RFP (chromatin, magenta), and HS-utrophin-GFP (F-actin, gray). Colored dots mark three daughter nuclei. Blue arrow marks a cytokinetic furrow that later regresses, and yellow arrows mark a cytokinetic furrow that divides three daughter nuclei into two cells. A mononucleated cell is marked with a white dot, and a binucleated cell is marked with a blue dot and a green dot. Frames are from Movie S2.

For all panels: HS was applied at 24 hpf, and imaging started at 10 hphs. Scale bars, 5 μm. Time is given in minutes.

See also Movies S1 and S2.

also, in OS-Plk4 p53 morphants, the majority of binucleated daughters died (61%; N = 20, n = 56). However, p53 knockdown did rescue some of the apoptotic phenotypes observed for mononucleated cells (Figure S5A). This raised the possibility that cell binucleation, per se, leads to apoptosis in the neuroepithelium.

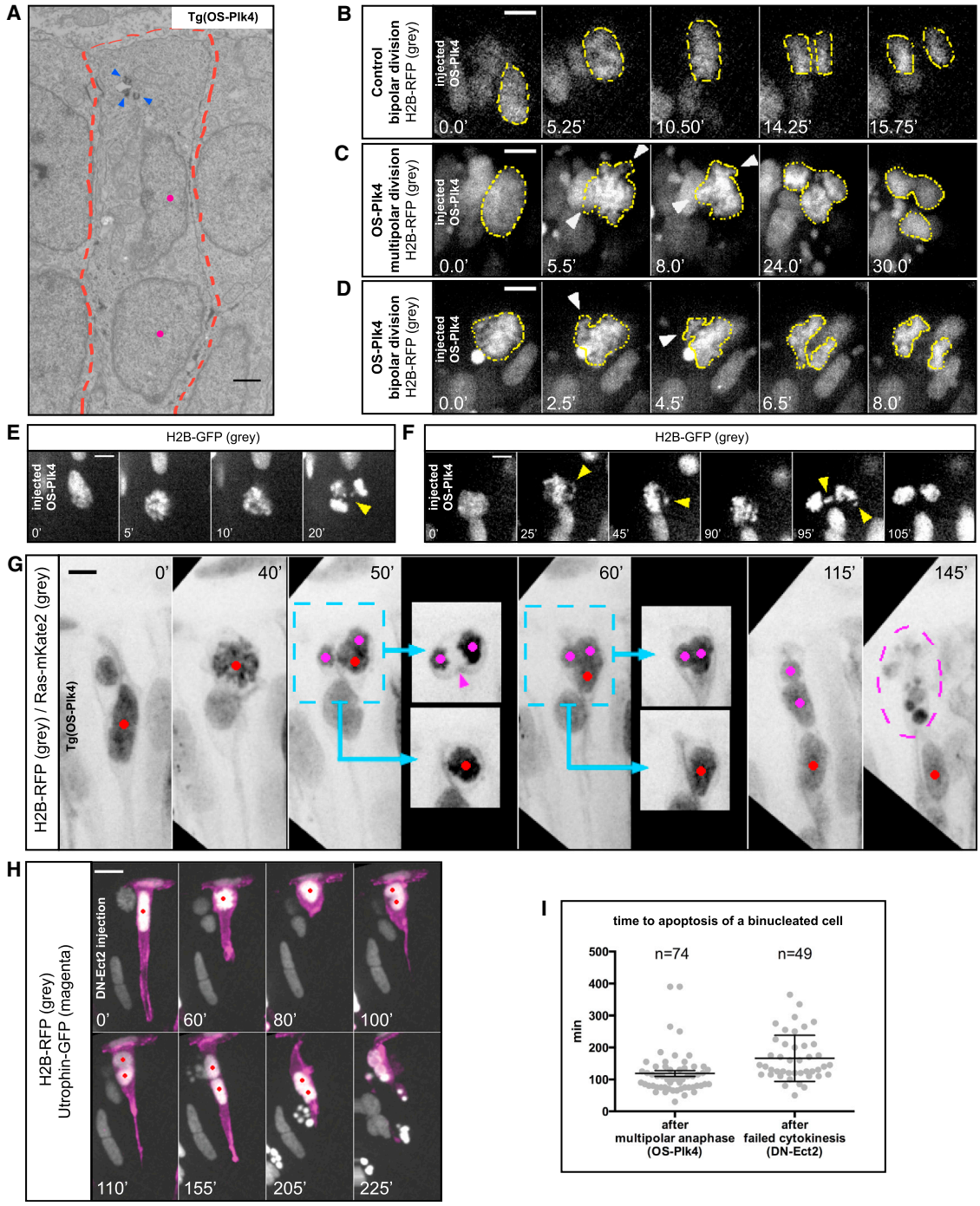

Figure 3. Upon Centriole Amplification, Cells Feature Genetic Material Distribution Defects at Mitosis, but Only the Generation of Binucleated Cells Triggers Apoptosis in Neuroepithelia

(A) EM image of a binucleated cell in the neuroepithelium of a Tg(HS-OS-Plk4) embryo. Arrows show amplified centrioles, dots indicate both nuclei, and cell outline is highlighted with a dashed line. Scale bar, 1 μm. HS was applied at 24 hpf and cells were fixed at 10 hphs.

(B) Time-lapse images of a neuroepithelial cell in a WT embryo exhibiting bipolar anaphase. HS-H2B-RFP labels chromatin (gray with yellow outlines). Frames are from Movie S3. HS was applied at 24 hpf, and imaging started at 14 hphs.

(C–F) Time-lapse images of a neuroepithelial cell in an embryo injected with HS-OS-Plk4, exhibiting multipolar (C and E) or bipolar (D and F) anaphase. HS-H2B-RFP labels chromatin (gray with yellow outlines). Arrows mark chromatin bursts and lagging chromosomes. Frames are from Movie S3. HS was applied at 24 hpf, and imaging started at 14 hphs.

(G) Time-lapse images of a neuroepithelial cell in a Tg(HS-OS-Plk4) embryo. H2B-RFP labels chromatin, and Ras-mKate2 labels cell outline (both in gray). A cell exhibits a multipolar anaphase. Colored dots mark three daughter nuclei. In the insets, the daughter nuclei are shown in two different z planes to distinguish a

(legend continued on next page)

To test this idea, we induced cell binucleation by interference with cytokinesis. To this end, we used a DN-Ect2 (Matthews et al., 2012) construct, as interference with Ect2 function has been shown to induce cytokinetic failure and generate binucleated cells in zebrafish epithelia (Hoijman et al., 2015). Indeed, this treatment resulted in binucleated daughter cells in the neuroepithelium (in these cells, however, each nucleus should feature the correct, diploid amount of genetic material). 87% (N = 15, n = 49) of these cells underwent apoptosis, with similar kinetics as those seen for binucleated daughters with centriole amplification upon OS-Plk4 expression (Figures 3H and 3I; Movie S4). This corroborates the idea that the generation of binucleated cells can be linked to the apoptotic response in the neuroepithelium.

Binucleation upon Multipolar Anaphase Does Not Lead to Apoptosis in Skin Cells

Detailed inspection of caspase-stained Tg(OS-Plk4) fish revealed that, while apoptosis was common in neuroepithelia, the otic vesicle, and the gut (Figure S5C), apoptotic cells were absent from the skin. To determine whether skin epidermal cells differ from other epithelial cells in their response to OS-Plk4 expression, we confirmed that, also in skin cells, OS-Plk4 expression leads to centriole amplification (Figure 4A). Furthermore, we established that earlier HS at 16 hpf did not lead to apoptotic events, as judged by caspase staining at 24 hphs (Figure S5D), excluding the possibility that we missed the time during which epidermal cells proliferate (Sonal et al., 2014). Next, we investigated how the genetic material is distributed in these cells. Following single-cell dynamics, we noted that, like in the neuroepithelial cells, OS-Plk4 expression in the epidermis led to bipolar as well as multipolar anaphases. Multipolar anaphase occurred in 1% of control epidermal cells (N = 4, n = 82) and in 25% of cells in the HS-OS-Plk4 line (N = 5, n = 69). As seen in the neuroepithelium (Figure 4B; Movie S5), cytokinesis in the epidermal cells always distributed the genetic material into two daughter cells, despite the initiation of multiple cleavage furrows. However, not a single skin cell underwent apoptosis after bipolar or multipolar anaphase (Figure S5A). Even when cells inherited two nuclear masses, they could enter another round of mitosis (Figure 4C; Movie S5). This implies that skin cells tolerate binucleation without apoptosis.

Centriole Amplification Affects the Proliferative Phase of Retinal Development but Not Neuronal Differentiation

So far, we showed that binucleation upon centriole amplification is linked to apoptosis in the neuroepithelium. In contrast, mononucleated cells in this tissue do not usually enter the apoptotic program (Figure S5A). We asked whether these mononucleated cells could enter another round of cell division. This was, indeed, the case, and such divisions occurred with bipolar or multipolar anaphases (Figures 5A–5C and S5B; Movie S6). This shows that mononucleated cells, upon OS-Plk4 expression, do not stall or exit the cell cycle. In contrast, they continue to proliferate, despite likely errors in chromosome segregation resulting from the presence of supernumerary centrioles (Figures 1D–1F, 3C–3F, and S2A–S2D; Movie S3). Interestingly, while imaging consecutive divisions of neuroepithelial cells expressing OS-Plk4, we found that the probability to retain anaphase configuration at the next mitosis was equal to the probability that it would change (Figure S5B). We also noted in our analysis of mitotic neuroepithelial cells labeled with centrin antibody that 74% of cells featuring a bipolar anaphase (n = 35) contained five centrioles or fewer. This was in contrast to cells with multipolar spindle configurations, as 83% of these cells were observed to contain six or more centrioles (n = 18). This suggests that, in the presence of fewer centrioles, the probability that a bipolar spindle will be formed is higher and that mitotic outcome following centriole amplification is correlated with the number of centrioles present in the cell.

Next, we wanted to investigate how OS-Plk4-driven centriole amplification impacts later retina development. For this, we performed HS on transgenic OS-Plk4 embryos at 24 hpf, and their retinae were analyzed at 80 hpf. All embryos showed disturbed retinal neuronal layer formation in comparison to controls (Figures 6A–6C). 48% of analyzed OS-Plk4 retinae (N = 33) displayed milder perturbations, in which some early neuronal layer formation was still detectable (marked by Zn5-positive retinal ganglion cells and apically localized photoreceptors) (Figure 6B). In the remaining 52% of embryos, retinal layering was severely impaired, with no distinct nuclear layer organization (Figure 6C). Notably, in both cases, retinae of transgenic OS-Plk4 fish featured holes, most likely resulting from cell death (Figures 6B and 6C). This indicates that the presence of supernumerary centrioles resulting from OS-Plk4 expression fundamentally affects retinal tissue development and maturation but that some cells can still enter neuronal fates. As our data suggested that centriole arrangements during mitosis are not an inherent property within a cell linage (Figure S5B), we speculated that any progenitor cell in the neuroepithelium faces a risk of undergoing a multipolar anaphase when supernumerary centrioles are present, and the more rounds of proliferation take place, the more apoptosis-prone, binucleated progeny would be generated. This, in turn, should lead to a more detrimental outcome for tissue development, the earlier centriole amplification is induced. To test this hypothesis, we performed HS at 16 hpf, when the optic cup has just been formed and retinal progenitors are established. Indeed, the

binucleated cell (magenta dots) and a mononucleated cell (red dot). Magenta arrow in the inset at time (t) = 50 min (50′) indicates a cytokinetic furrow that later regresses, resulting in the formation of a binucleated daughter. Dashed circle at t = 145′ marks apoptosis of the binucleated cell. Frames are from Movie S4. HS was applied at 24 hpf, and imaging started at 10 hphs.

(H) Time-lapse images of a neuroepithelial cell in a WT embryo injected with HS-DN-Ect2. HS-H2B-RFP labels chromatin (gray), and HS-utrophin-GFP labels F-actin (magenta). The red dot marks a single nucleus before division and two nuclei in a respective cell after failed cytokinesis at t = 100′. The frames are from Movie S4. Scale bar, 10 μm. HS was applied at 32 hpf, and imaging started at 2 hphs.

(I) Time between completion of division and apoptosis of binucleated cells. Analysis on WT embryos injected with HS-OS-Plk4 (multipolar anaphase) and HS-DN-Ect2 (failed cytokinesis). Each dot represents one binucleated cell that underwent apoptosis. Lines represent mean ± SEM.

Scale bars, 5 μm unless otherwise stated. Time is given in minutes.

See also Movies S3 and S4.

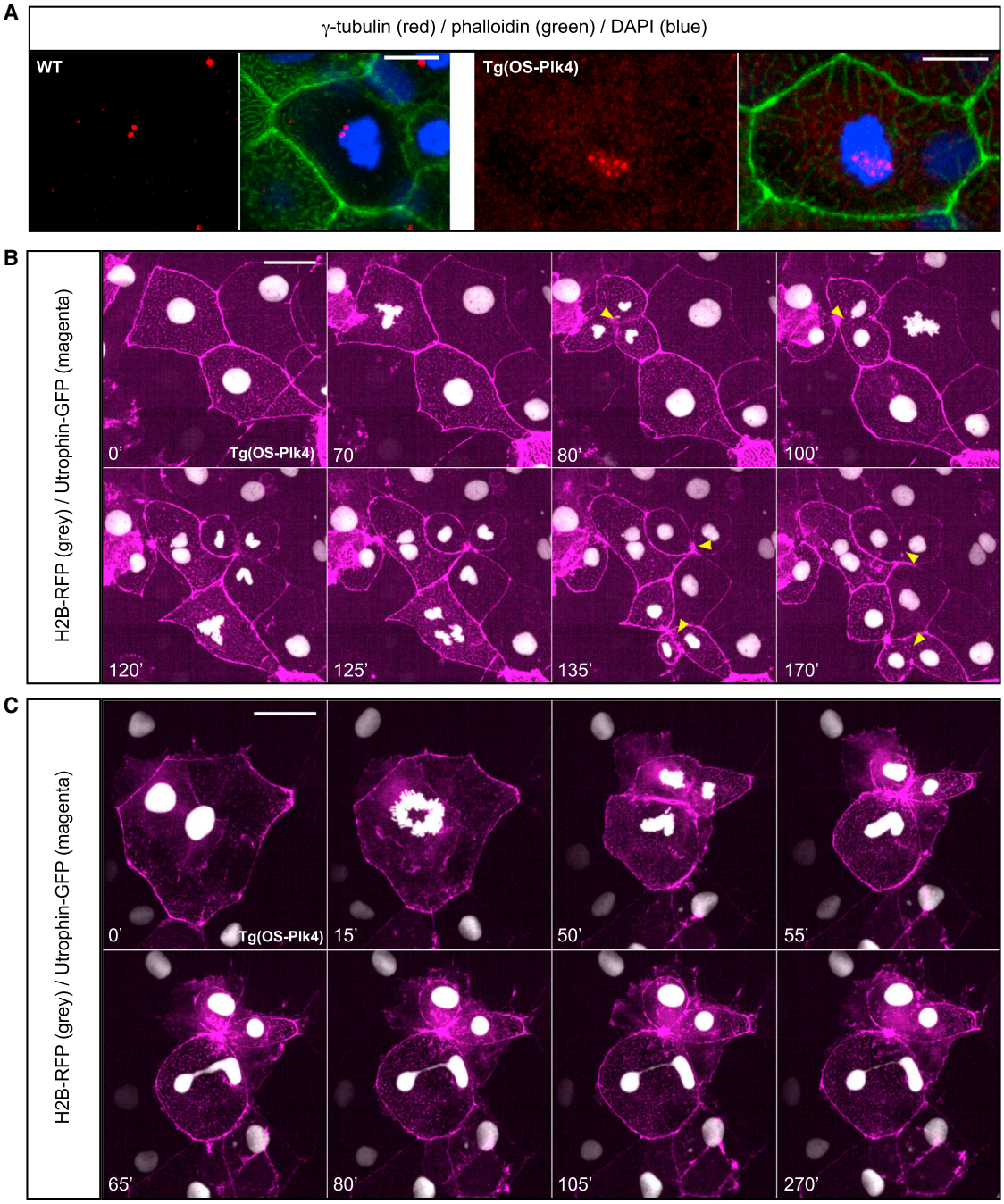

Figure 4. In Skin Cells, Binucleation upon Multipolar Anaphase Does Not Lead to Apoptosis

(A) A confocal scan of a WT epidermal cell (left) with two γ-tubulin foci (red) and a epidermal cell in a Tg(HS-OS-Plk4) embryo (right) with six γ-tubulin foci (red). Merged with cell outlines (phalloidin, green) and chromatin (DAPI, blue). Scale bars, 20 μm. HS was applied at 16 hpf, and embryos were fixed at 12 hphs.

(B) Time-lapse images of three epidermal cells in a Tg(HS-OS-Plk4) embryo undergoing multipolar anaphases. Krt8-H2B-RFP labels chromatin (gray), and HS-utrophin-GFP labels F-actin (magenta). Initially, two cytokinetic furrows (arrows) are established, but later, one of them regresses, generating binucleated daughters. Frames are from Movie S6.

(C) Time-lapse images of a binucleated epidermal cell in a Tg(HS-OS-Plk4) embryo undergoing a multipolar anaphase. Krt8-H2B-RFP labels chromatin (gray), and HS-utrophin-GFP labels F-actin (magenta). The cell enters mitosis and divides, generating two binucleated daughters. Frames are from Movie S6.

For (B) and (C): HS was applied at 16 hpf, and imaging started at 8 hphs. Scale bars, 25 μm. Time is given in minutes.

See also Movie S6.

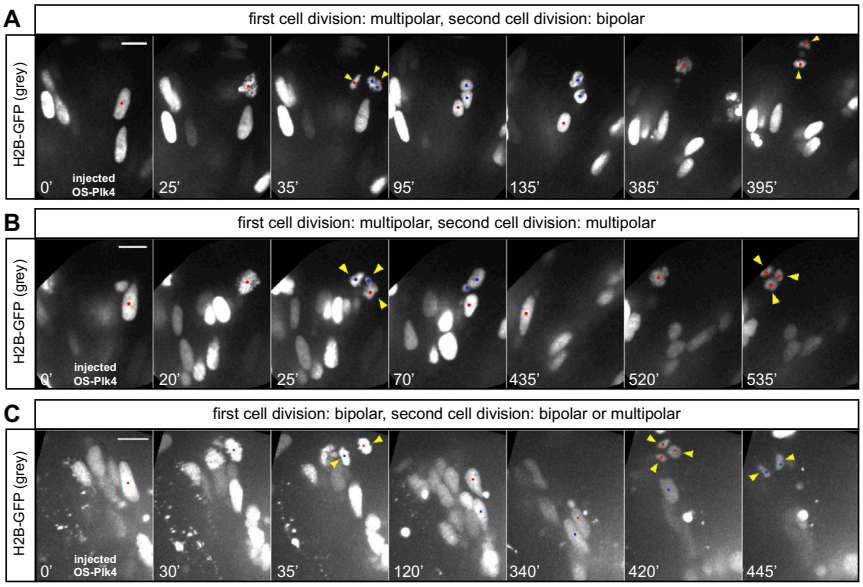

Figure 5. Mononucleated Neuroepithelial Cells Generated upon Division in the Presence of Supernumerary Centrioles Can Re-enter Mitosis with Bipolar or Multipolar Anaphases

(A) Time-lapse images of a neuroepithelial cell in a WT embryo injected with HS-OS-Plk4. H2B-GFP labels chromatin (gray). A cell exhibits a multipolar anaphase at time (t) = 35 min (35′) (arrows). A binucleated daughter cell (marked with two blue dots) undergoes apoptosis at t = 135′. A mononucleated cell (marked with a red dot) enters a second mitosis, exhibiting a bipolar anaphase at t = 395′ (arrows). Frames are from Movie S6.

(B) Time-lapse images of a neuroepithelial cell in a WT embryo injected with HS-OS-Plk4. H2B-GFP labels chromatin (gray). A cell undergoes a multipolar anaphase at t = 25′ (arrows). A mononucleated daughter cell (marked with a red dot) enters a second mitosis, exhibiting a multipolar anaphase at t = 535′ (arrows). Frames are from Movie S6.

(C) Time-lapse images of a neuroepithelial cell in a WT embryo injected with HS-OS-Plk4. H2B-GFP labels chromatin (gray). A cell undergoes a bipolar anaphase at t = 35′ (arrows). Both daughter cells enter next cell division, exhibiting a multipolar (marked with red dots) or bipolar (marked with blue dots) anaphase (arrows at t = 420′ and 445′). Frames are from Movie S6.

For all panels: HS was applied at 24 hpf, and imaging started at 10 hphs, Scale bar, 10 μm. Time is given in minutes.

See also Movie S6.

defects observed in these fish were more drastic than for the 24 hpf HS: the retinae were smaller, and 83% of analyzed eyes (N = 24) displayed a severe phenotype without any distinct nuclear or neuronal layering (Figure 6D). This suggests that overall development of the retinal tissue in the presence of supernumerary centrioles can be correlated with the proliferative capacity of the progenitor cells and that retinal development is particularly sensitive to centriole amplification during the proliferative phase.

As we observed that some neuronal layering could still be established upon OS-Plk4 expression (Figure 6B), we next wondered how exactly centriole amplification impacts neuronal differentiation. Crossing OS-Plk4 fish to transgenic lines labeling both early (Ath5-gapRFP marker for retinal ganglion and photoreceptors) and later-born neurons (Ptf1A-GFP marker for amacrine and horizontal cells and Vsx1-GFP marker for bipolar cells) (Weber et al., 2014) revealed that OS-Plk4-expressing cells were able to differentiate into all neuronal subtypes (Figures 6E and 6F). To test whether this was also the case upon mosaic expression, we injected the HS-OS-Plk4 construct together with the HS-H2B-GFP to label Plk4-expressing cells. We found that H2B-positive cells integrated into the tissue and contributed to the formation of all neuronal layers (Figure 6G; N = 18).

To further exclude the possibility that OS-Plk4-expressing cells show defects in the neuronal differentiation program, we inspected OS-Plk4 transgenic fish expressing Ath5-gapRFP and Ptf1A-GFP at the onset of neurogenesis. We did not observe significant differences between OS-Plk4-expressing and control embryos in terms of the timing of differentiation into early- or later-born neurons. This suggests that the birth order of neurons is conserved in OS-Plk4-expressing fish and that no premature differentiation occurs (Figure 6H; N = 4 for both, OS-Plk4 and WT). These data, together with our observation that OS-Plk4-expressing cells can undergo multiple rounds of division (Figures 5A–5C and S5B), argue that no precocious cell cycle exit of retinal progenitors takes place upon OS-Plk4 expression. On the contrary, when cells do not undergo apoptosis beforehand, they can undergo timely differentiation into all neuronal cell types and take part in the formation of all neuronal layers.

To ensure that these differentiated neurons still contain multiple centrioles, we performed EM analysis on fish showing neuronal differentiation, visualized by Ath5-RFP expression. We focused on cells localized at the basal region of the retinal tissue, where differentiated neurons reside at this developmental stage. As expected, in control cells (N = 1, n = 5), we always detected two centrioles, indicating that these cells contain a single, non-duplicated centrosome (Figure S6A). However, 57% of cells in transgenic OS-Plk4 fish (N = 3, n = 14) exhibited three or four clearly visible centrioles (Figure S6B). This confirms that cells in the OS-Plk4 condition can differentiate, despite the presence of aberrant centriole numbers.

As we observed that proliferation, but not differentiation, of retinal progenitor cells is affected by OS-Plk4 expression, we speculated that centriole amplification should have milder effects when induced at later developmental stages. To test this notion, we performed HS on transgenic embryos at 48 hpf. At this stage, neurogenesis peaks, and only few proliferative divisions remain (Weber et al., 2014). Indeed, in these fish, retinal development was not significantly impaired: all retinal layers were formed, largely resembling control retinae, and only minor defects could be observed (Figures 6I [N = 7] and 6J [N = 9]).

Collectively, these data suggest that the bottleneck for successful retinal maturation upon OS-Plk4-driven centriole

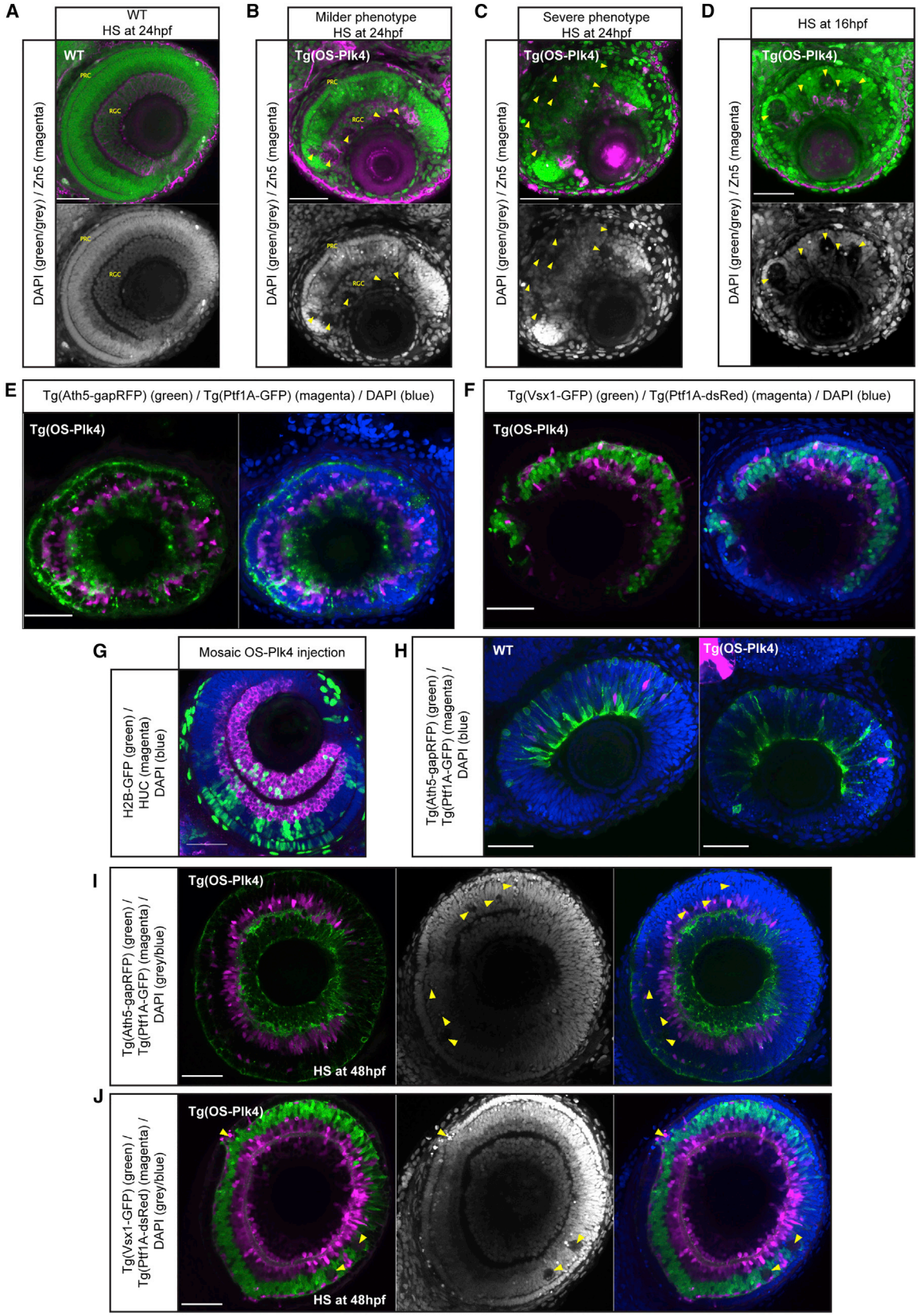

(legend on next page)

amplification is cell proliferation. In contrast, supernumerary centrioles are not a major hindrance for timely differentiation into all neuronal subtypes at later developmental stages.

WT Cells Can Compensate for Apoptotic Cell Loss Resulting from Centriole Amplification

We showed that transgenic OS-Plk4 fish displayed extensive apoptosis and tissue degeneration upon centriole amplification (Figures 1C and 1G). These effects were much less severe in fish injected with the HS-OS-Plk4 construct (Figure S2E). One explanation for this difference could be that, upon injection, only a subset of cells expressed OS-Plk4 and, consequently, fewer cells underwent apoptosis. Furthermore, it was previously shown that retinal cells feature remarkable compensatory capabilities and can counteract the loss of cells by additional and ectopic proliferation (Weber et al., 2014). We tested whether such compensation also takes place in HS-OS-Plk4-injected embryos. To this end, we stained control and OS-Plk4-injected embryos for the mitotic marker pH3. In the control, some proliferation took place at apical and subapical regions at 80 hpf, but only 27% of embryos showed relatively high pH3 signal at these locations (Figure 7A; N = 15). On the other hand, the fish injected with HS-OS-Plk4 exhibited higher proliferative activity, with 63% of embryos showing high pH3 signal. Additionally, 24% of embryos showed abnormal, ectopic proliferation, which was never observed in the control (Figure 7B; N = 21). This argues that, indeed, cell loss due to apoptosis can trigger additional proliferation.

To understand the extent to which WT cells can compensate for cell loss, we used cell transplantation to introduce small populations of WT cells into the OS-Plk4 background. Transplanted OS-Plk4 fish often had eyes of noticeably different sizes (Figures 7C, S7A, and S7B). Remarkably, when both eyes were imaged, transplanted cells appeared to have repopulated the retina in the more normal looking larger eye and largely restored retinal morphology and neuronal layering (Figures 7D, left panel and S7C and S7D, top panels). In contrast, the smaller eye contained few or no transplanted cells and displayed practically no retinal layering (Figures 7D, middle panels and S7C and S7D, middle panels). This indicates that WT cells can significantly rescue the phenotypes induced by centriole amplification, possibly by compensatory proliferation. The fact that such large numbers of offspring of transplanted cells were never observed when cells were transplanted into a WT background further supports this notion (Figures 7D, right panel and S7C and S7D, lower panels). Taken together, these results represent one of the most striking examples, to date, of compensation for retinal cell loss.

DISCUSSION

In this study, we investigated the cellular basis of how centriole amplification induced by OS-Plk4 overexpression impacts tissue and organismal development focusing on zebrafish neuroepithelia. Our study reveals that centriole amplification induces multipolar anaphases and that these lead to the formation of binucleated daughter cells. Such binucleation is linked to apoptosis in the neuroepithelium. Not all epithelia are equally sensitive to centriole amplification, however, as skin cells tolerate binucleation without apoptosis. We further provide evidence that the risk for binucleation occurs at every cell division, with supernumerary centrioles leading to more severe consequences when centriole amplification is induced earlier in development. However, despite the presence of supernumerary centrioles, neuroepithelial cells are able to undergo timely differentiation into all neuronal subtypes. Finally, we find that the presence of WT cells within a population of cells with amplified centrioles can compensate for apoptotic cell loss and significantly restore retinal tissue organization.

The Generation of Binucleated Cells Induces Apoptosis in the Neuroepithelium

Centriole amplification in zebrafish epithelia can result in bipolar or multipolar anaphase. Both of these anaphase configurations can lead to erroneous distribution of genetic material. In the neuroepithelium, cell death mostly occurs following multipolar anaphase and can be linked to the generation of binucleated daughter cells. A similar apoptotic response is seen upon

Figure 6. Centriole Amplification Affects the Proliferative Phase of Retinal Development but Not Neuronal Differentiation

(A–C) Confocal scans of the retinae of control (A) and transgenic Tg(HS-OS-Plk4) fish (B and C) showing milder (B) or severe (C) phenotypes; HS was applied at 24 hpf, and these embryos were fixed at 80 hpf and stained for Zn-5 (retinal ganglion cells, or RGCs; magenta) and DAPI (nuclei, green/gray). Arrows label holes in nuclear arrangement. In fish with milder phenotype (B), some neuronal layering can be observed corresponding to RGC layer and photoreceptor cell (PRC) layer.

(D) Confocal scan of the retina of a Tg(HS-OS-Plk4) fish; HS was applied at 16 hpf, and these embryos were fixed at 80 hpf and stained for Zn-5 (magenta) and DAPI (green/gray). Arrows label large holes in the tissue.

(E) Confocal scan of the retina of Tg(HS-OS-Plk4) fish crossed to Tg(Ath5-gapRFP) (marker of early born neurons: RGCs and PRCs, green) and Tg(Ptf1A-GFP) (marker of later born neurons: amacrine and horizontal cells, magenta) line; HS was applied at 24 hpf, and these embryos were fixed at 76 hpf and stained for DAPI.

(F) Confocal scan of the retina of Tg(HS-OS-Plk4) fish crossed to Tg(Vsx1-GFP) (marker of late-born bipolar cells, green) and Tg(Ptf1A-dsRed) (magenta) lines, HS was applied at 24 hpf, and these embryos were fixed at 96 hpf and stained for DAPI.

(G) Confocal scan of the retina of fish injected with HS-OS-Plk4 construct and HS-H2B-GFP construct (labeling OS-Plk4-expressing cells, green); HS was applied at 24 hpf, and these embryos were fixed at 80 hpf and stained for HuC/D (RGCs and amacrine cell marker, magenta) and DAPI (blue).

(H) Confocal scans of retinae from crosses of Tg(HS-OS-Plk4) fish to Tg(Ath5-gapRFP) (green) and Tg(Ptf1A-GFP) (magenta) lines (right panel) and Tg(Ath5-gapRFP) (green)/Tg(Ptf1A-GFP) (magenta) line only (control, left panel); HS was applied at 24 hpf, and these embryos were fixed at 50 hpf and stained for DAPI (blue).

(I and J) Confocal scan of the retina of Tg(HS-OS-Plk4) fish crossed to the Tg(Ath5-gapRFP) (green)/Tg(Ptf1A-GFP) (magenta) line (I) or Tg(Vsx1-GFP) (green)/Tg(Ptf1A-dsRed) (magenta) line (J). HS was applied at 48 hpf, and these embryos were fixed at 78 hpf and stained for DAPI (gray/blue). Arrows point at smaller holes/apoptotic regions in the tissue.

Scale bars, 50 μm.

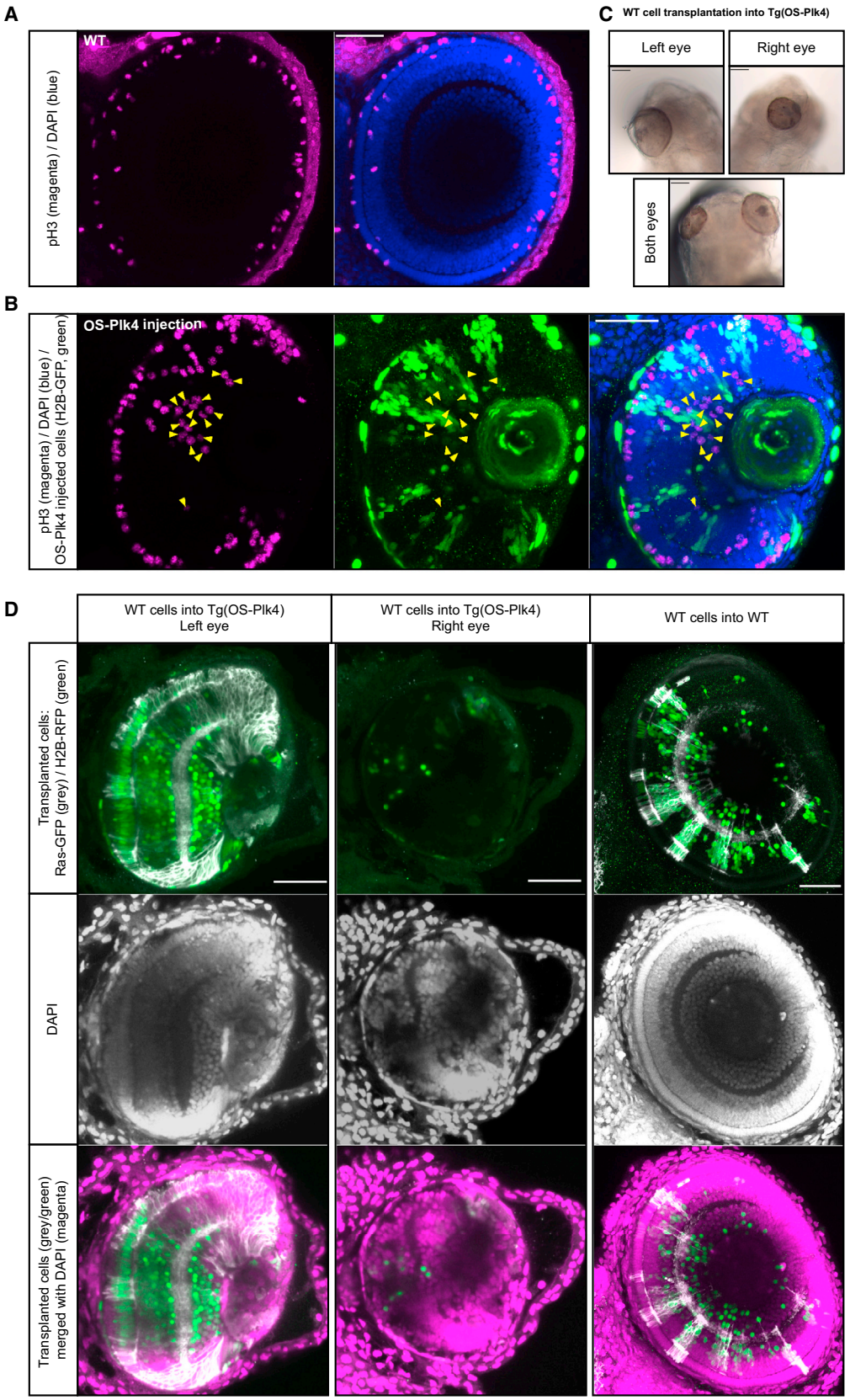

(legend on next page)

interference with cytokinesis, which also leads to the formation of binucleated cells. This indicates that neural progenitors are sensitive to binucleation independently of its cause. Thus, it is most likely not the misdistribution of genetic material, per se, that leads to cell death in the zebrafish neuroepithelium but specifically the generation of binucleated cells.

Skin Cells Tolerate Centriole Amplification and Binucleation

It became previously apparent that not all epithelia respond the same to centriole amplification (Marthiens et al., 2013; Sabino et al., 2015). Unlike cells in the neuroepithelium, we found that cells of the zebrafish skin epidermis do not undergo apoptosis in response to centriole amplification. This indicates that skin cells cope differently with the presence of supernumerary centrioles and subsequent binucleation. One possible explanation for this observed robustness could be that substantial apoptosis at the surface of the developing animal would open the organism to a multitude of pathogens and other harmful substances in its environment. Such an exposure must most likely be avoided at all costs, even when it results in cells with abnormal amounts of genetic material and nuclear number. It will be interesting to explore whether such retention of cells with abnormal genetic content has any deleterious consequences, such as tumorigenesis, at later developmental stages.

Centriole Amplification Is Particularly Detrimental during the Proliferative Phase of Retinal Development but Does Not Hinder Neuronal Differentiation

We show that, upon centriole amplification in the neuroepithelium, bipolar or multipolar anaphases occur with almost equal probability at any given division. Furthermore, anaphase configurations are not conserved in consecutive cell cycles. This is comparable to a coin toss, taking place at each round of division, deciding whether daughter cells will survive or die. Consequently, the more cell cycles a neuroepithelial cell enters, the more likely it becomes that this cell will eventually generate a binucleated, apoptotic daughter. In support of this idea, we demonstrate that retinal maturation defects are exacerbated when supernumerary centrioles are induced early during retinogenesis and are less pronounced when centriole amplification is induced at later developmental stages.

It has been reported that centriole amplification in the mouse leads to premature cell cycle exit of neural progenitors, contributing to the observed microcephaly phenotype (Marthiens et al., 2013). However, retinal neuroepithelial cells are able to undergo timely differentiation into all neuronal cell types and are found in all neuronal layers upon centriole amplification. Importantly, the combination of our study and previous studies implies that centriole amplification can have divergent effects on different organisms and tissues. It will now be important to understand the origins of these remarkable differences.

WT Cells Can Compensate for Cell Death Induced by Centriole Amplification

We find that tissue defects are significantly milder following mosaic induction of centriole amplification than in animals with ubiquitous perturbation. This would be expected, as fewer cells feature amplified centrioles in mosaic animals. However, our results indicate that this is not the only reason for improved tissue maintenance. In addition, cells that are not affected by the perturbation seem to proliferate more, often at ectopic positions and thereby provide compensation for cell loss. We find that such compensation is even possible when relatively few WT cells are present in the transplantation scenario. The offspring of these transplanted cells can rescue many of the defects, including neuronal layering. Compensation phenotypes by increased and ectopic proliferation in the zebrafish retina were previously observed when specific neuronal subtypes were prevented from forming (Weber et al., 2014). Compensation for cell death also occurs upon centriole depletion in the *Drosophila* wing epithelium (Poulton et al., 2014). Altogether, these findings argue that forming a normally organized tissue is of utmost importance for the organism. It will be very interesting to investigate how cell compensation is triggered upon perturbations, including cell loss, and how it is shut down once general tissue organization has been restored.

Overall, this study provides significant cellular insights into how centriole amplification impacts neural tissue in the developing zebrafish, complementing and expanding previous studies in *Drosophila* and the mouse (Basto et al., 2008; Sabino et al., 2015; Marthiens et al., 2013). Continued studies on the effects of centriole amplification in different tissues and model organisms will provide an even deeper understanding of centrosome biology and how centriole amplification leads to disease scenarios. One implication that arises from the combination of the studies to date is that in none of the investigated developing tissues was primary tumorigenesis observed. This could mean that centriole amplification is not a significant trigger for cancer emergence during development. However, it is possible that mature tissues are more prone to cancer initiation upon centriole amplification. It will be of major importance to follow up on these questions in future studies.

Figure 7. WT Cells Can Compensate for Apoptotic Cell Loss Resulting from Centriole Amplification

(A and B) Confocal scans of the retina of a WT fish (A) and a fish injected with HS-OS-Plk4 and HS-H2B-GFP constructs (green) (B); HS was applied at 24 hpf, and these embryos were fixed at 80 hpf and stained for phospho-histone 3 (pH3) (mitotic cells, magenta) and DAPI (nuclei, blue). Arrows point at mitotic cells at ectopic positions.

(C) Bright-field images of the eyes of Tg(HS-OS-Plk4) fish transplanted with WT cells. Scale bar, 100 μm.

(D) Confocal scans of the retinae of fish following transplantation of WT cells, expressing Ras-GFP (gray) and HS-H2B-RFP (green). Left and middle panels show Tg(HS-OS-Plk4) fish depicted in (C). Right panel shows a WT transplanted fish (control); HS was applied at 24 hpf, and these embryos were fixed 2.5 days later (control)/4 days later in OS-Plk4 background to compensate for developmental delay and stained with DAPI (gray/magenta).

Scale bars, 50 μm unless otherwise stated.

See also Figure S7.

EXPERIMENTAL PROCEDURES

Zebrafish Husbandry

Strains used in this study: WT AB and TL; Tg(HS-OS-Plk4-mKate2) and Tg(HS-H2B-RFP) (both used in this study; see Supplemental Experimental Procedures for details); Tg(Vsx1-GFP), Tg(Ptf1a-dsRed), Tg(Ptf1a-GFP), and Tg(Ath5-gapRFP) (all in Weber et al., 2014); and Tg(β-actin-Ras-GFP) (a kind gift from C.P. Heisenberg).

Zebrafish were maintained and bred at 26.5°C. Embryos were raised at 28°C. Embryos were treated with 0.003% phenylthiourea (Sigma) from 10 hpf to prevent pigmentation. All animal work was performed in accordance with European Union (EU) directive 2011/63/EU, as well as the German Animal Welfare Act.

Centriole Amplification Strategy

To achieve centriole amplification, human Plk4 containing a deletion of amino acids 282–305 required for autophosphorylation and degradation was expressed (Holland and Cleveland, 2012). This construct was placed under the HS promoter generating HS-OS-Plk4-mKate2 (Strzyz et al., 2015). To achieve mosaic expression, this construct was injected into one-cell-stage embryos. In order to yield ubiquitous expression, a Tg(HS-OS-Plk4-mKate2) line was generated.

HS of Embryos

To induce expression from the HS-promoter-driven constructs, Petri dishes with embryos were placed in a 39°C water bath for 30 min. HS was performed at 24 hpf unless otherwise stated.

Apoptosis Detection by Acridine Orange

Dechorionated embryos were incubated in a 2 μg/ml solution of acridine orange (Sigma) in PBS for 30 min at room temperature. Embryos were rinsed 5× in E3 and then were washed 5× for 5 min in E3 and subsequently observed under the fluorescent stereomicrosope using a GFP filter set.

Constructs Used

The following constructs, labeling intracellular structures, were used: HS-H2B-RFP, HS-utrophin-GFP, and pCS2+ Ras-mKate2 (all in Strzyz et al., 2015); pCS2+ centrin-GFP and pCS2+ H2B-RFP (both in Norden et al., 2009); HS-H2B-GFP, keratin 8 (krt8)-H2B-RFP, and HS-DN-Ect2 (all three in this study; see Supplemental Experimental Procedures for details).

p53 Knockdown

To knock down the p53 expression, p53 morpholino was used (GeneTools, 5′-GCGCCATTGCTTTGCAAGAATTG-3′). Injection of 3 ng per embryo was performed at the one-cell stage.

DNA/RNA Injections and Transplantations

DNA constructs were injected in a 0.5- to 1-nl volume, at a concentration of 10 ng/μl per construct, into the cytoplasm of one-cell-stage embryos. RNA was synthesized using the Ambion SP6 mMessage Machine kit and injected in 0.3- to 0.6-nl concentrations into one or two cells of 16- to 64-cell-stage embryos at concentrations of 50–125 ng/μl per construct. In experiments in which injected fish were kept until 80 hpf, p53 morpholino was co-injected to facilitate retention of injected cells in the tissue. Transplantations were performed as previously described (Weber et al., 2014).

Immunofluorescence

Embryos were fixed overnight in 4% paraformaldehyde at 4°C. Whole-mount staining was carried out as previously described (Norden et al., 2009). For a list of antibodies, see the Supplemental Experimental Procedures.

In Vivo Time-Lapse Imaging

Embryos were anesthetized using 0.04% MS-222 (Sigma) and mounted in 1% low-melt agarose in E3 medium on Mattek glass-bottom dishes. An Andor spinning disc system with a 63× water immersion objective (NA = 1.2) and a 30°C heating chamber was used. z stacks of 28–35 μm were collected, with 1-μm optical sections. Images were acquired every 5 min (unless otherwise stated) for 10–14 hr.

Confocal Scans

Imaging was performed on Zeiss LSM 510 or 710 confocal microscopes with a Zeiss 40× water-immersion objective (NA = 1.1-1.2). Image analysis was performed using ImageJ/Fiji software (NIH).

Conventional Transmission EM

Zebrafish embryos at 30–36 hpf (WT or OS-Plk4) were fixed in 1% glutaraldehyde, 1% paraformaldehyde in buffer, as described by Seiler and Nicolson (1999), for 2 days, followed by a standard procedure (see Supplemental Experimental Procedures for details). Alignment of the serial micrographs and 3D reconstruction was performed with the TrakEM2 plugin (Cardona et al., 2012) in the ImageJ-based free software Fiji.

Statistical Analyses

A two-tailed unpaired t test assuming equal SD was performed using GraphPad Prism, version 6.0f for Mac OS X, GraphPad software. On graphs, means and SEM are shown unless otherwise stated.

SUPPLEMENTAL INFORMATION

Supplemental Information includes Supplemental Experimental Procedures, seven figures, and six movies and can be found with this article online at http://dx.doi.org/10.1016/j.celrep.2015.08.062.

AUTHOR CONTRIBUTIONS

P.J.S. and C.N. conceived the study. E.D. and P.J.S. performed all experiments and analysis except for EM. M.W.-B. performed the EM analysis. C.N., P.J.S., and E.D. wrote the manuscript.

ACKNOWLEDGMENTS

We thank the C.N. lab and J. Mansfeld, J. Huisken, I.K. Patten, and B. Cheeseman for discussion and helpful comments on the manuscript. S. Schneider, H.O. Lee, J. Sidhaye, and the MPI-CBG Fish and Light Microscopy Facility are thanked for experimental help. We are grateful to W.B. Huttner for experimental support. We further thank C.P. Heisenberg and S. Narumiya for sharing constructs and fish lines. C.N. is supported by the Human Frontier Science Program (CDA-00007/2011) and the German Research Foundation (DFG).

Received: June 1, 2015
Revised: August 5, 2015
Accepted: August 21, 2015
Published: September 24, 2015

REFERENCES

Alderton, G.K., Galbiati, L., Griffith, E., Surinya, K.H., Neitzel, H., Jackson, A.P., Jeggo, P.A., and O'Driscoll, M. (2006). Regulation of mitotic entry by microcephalin and its overlap with ATR signalling. Nat. Cell Biol. *8*, 725–733.

Basto, R., Brunk, K., Vinadogrova, T., Peel, N., Franz, A., Khodjakov, A., and Raff, J.W. (2008). Centrosome amplification can initiate tumorigenesis in flies. Cell *133*, 1032–1042.

Cardona, A., Saalfeld, S., Schindelin, J., Arganda-Carreras, I., Preibisch, S., Longair, M., Tomancak, P., Hartenstein, V., and Douglas, R.J. (2012). TrakEM2 software for neural circuit reconstruction. PLoS ONE *7*, e38011–e38018.

Fırat-Karalar, E.N., and Stearns, T. (2014). The centriole duplication cycle. Philos. Trans. R. Soc. Lond. B: Biol. Sci. *369*, 20130460.

Ganem, N.J., Godinho, S.A., and Pellman, D. (2009). A mechanism linking extra centrosomes to chromosomal instability. Nature *460*, 278–282.

Habedanck, R., Stierhof, Y.-D., Wilkinson, C.J., and Nigg, E.A. (2005). The Polo kinase Plk4 functions in centriole duplication. Nat. Cell Biol. *7*, 1140–1146.

Hoijman, E., Rubbini, D., Colombelli, J., and Alsina, B. (2015). Mitotic cell rounding and epithelial thinning regulate lumen growth and shape. Nat. Commun. *6*, 7355.

Holland, A.J., and Cleveland, D.W. (2012). Losing balance: the origin and impact of aneuploidy in cancer. EMBO Rep. *13*, 501–514.

Holland, A.J., Lan, W., Niessen, S., Hoover, H., and Cleveland, D.W. (2010). Polo-like kinase 4 kinase activity limits centrosome overduplication by autoregulating its own stability. J. Cell Biol. *188*, 191–198.

Kimmel, C.B., Ballard, W.W., Kimmel, S.R., Ullmann, B., and Schilling, T.F. (1995). Stages of embryonic development of the zebrafish. Dev. Dyn. *203*, 253–310.

Langheinrich, U., Hennen, E., Stott, G., and Vacun, G. (2002). Zebrafish as a model organism for the identification and characterization of drugs and genes affecting p53 signaling. Curr. Biol. *12*, 2023–2028.

Leung, L., Klopper, A.V., Grill, S.W., Harris, W.A., and Norden, C. (2011). Apical migration of nuclei during G2 is a prerequisite for all nuclear motion in zebrafish neuroepithelia. Development *138*, 5003–5013.

Marthiens, V., Rujano, M.A., Pennetier, C., Tessier, S., Paul-Gilloteaux, P., and Basto, R. (2013). Centrosome amplification causes microcephaly. Nat. Cell Biol. *15*, 731–740.

Matthews, H.K., Delabre, U., Rohn, J.L., Guck, J., Kunda, P., and Baum, B. (2012). Changes in Ect2 localization couple actomyosin-dependent cell shape changes to mitotic progression. Dev. Cell *23*, 371–383.

Meraldi, P., and Nigg, E.A. (2002). The centrosome cycle. FEBS Lett. *521*, 9–13.

Nigg, E.A., Čajánek, L., and Arquint, C. (2014). The centrosome duplication cycle in health and disease. FEBS Lett. *588*, 2366–2372.

Norden, C., Young, S., Link, B.A., and Harris, W.A. (2009). Actomyosin is the main driver of interkinetic nuclear migration in the retina. Cell *138*, 1195–1208.

Pihan, G.A., Purohit, A., Wallace, J., Malhotra, R., Liotta, L., and Doxsey, S.J. (2001). Centrosome defects can account for cellular and genetic changes that characterize prostate cancer progression. Cancer Res. *61*, 2212–2219.

Poulton, J.S., Cuningham, J.C., and Peifer, M. (2014). Acentrosomal Drosophila epithelial cells exhibit abnormal cell division, leading to cell death and compensatory proliferation. Dev. Cell *30*, 731–745.

Sabino, D., Gogendeau, D., Gambarotto, D., Nano, M., Pennetier, C., Dingli, F., Arras, G., Loew, D., and Basto, R. (2015). Moesin is a major regulator of centrosome behavior in epithelial cells with extra centrosomes. Curr. Biol. *25*, 879–889.

Seiler, C., and Nicolson, T. (1999). Defective calmodulin-dependent rapid apical endocytosis in zebrafish sensory hair cell mutants. J. Neurobiol. *41*, 424–434.

Sonal, S., Sidhaye, J., Phatak, M., Banerjee, S., Mulay, A., Deshpande, O., Bhide, S., Jacob, T., Gehring, I., Nuesslein-Volhard, C., and Sonawane, M. (2014). Myosin Vb mediated plasma membrane homeostasis regulates peridermal cell size and maintains tissue homeostasis in the zebrafish epidermis. PLoS Genet. *10*, e1004614–e1004619.

Strzyz, P.J., Lee, H.O., Sidhaye, J., Weber, I.P., Leung, L.C., and Norden, C. (2015). Interkinetic nuclear migration is centrosome independent and ensures apical cell division to maintain tissue integrity. Dev. Cell *32*, 203–219.

Weber, I.P., Ramos, A.P., Strzyz, P.J., Leung, L.C., Young, S., and Norden, C. (2014). Mitotic position and morphology of committed precursor cells in the zebrafish retina adapt to architectural changes upon tissue maturation. Cell Rep. *7*, 386–397.